A STUDY ABOUT CELL ACTIVITY ON ANODIZED Ti-6Al-4V BY MEANS OF PULSED CURRENT

LUANA M. R. VASCONCELLOS[1], MARIA F. L. VILLAÇA-CARVALHO[1], RENATA F. PRADO[1], EVELYN L. S. L. SANTOS[1], NATAL N. REGONE[2], MARINALDA C. PEREIRA[3], EDUARDO N. CODARO[3], HELOISA A. ACCIARI[3,*]

[1]Institute of Science and Tecnology, São José dos Campos Campus, UNESP
[2]São João da Boa Vista Campus, UNESP
[3]Faculty of Engineering, Guaratinguetá Campus, UNESP, 333 Dr. Ariberto Pereira da Cunha Ave, CEP 12516-410, Guaratinguetá, SP, Brazil
*Corresponding Author: heloisa@feg.unesp.br

Abstract

Titanium and some of its alloys exhibit excellent anti-corrosive and biocompatibility properties due to rapid formation of a passive film on their surfaces when exposed to the atmosphere. However, such materials present poor osteoindutive properties. Surfaces modified via anodization are being proposed in this study to promote a chemical interaction between implants and bone cells. For this purpose, samples in Ti-6Al-4V alloy discs were anodized in a phosphoric acid solution using pulsed current for being applied in orthopaedic implants. The pulsed current is based on duty cycle (DC), which was supplied by a square wave pulse rectifier at 100 Hz and maximum tension of 30 V. A scanning electron microscope was used to obtain images of the anodized surfaces, thus revealing the presence of uniformly distributed pores over the entire surface, measuring approximately 2 μm in diameter. Osteogenic cells grown on the surface of the control and anodized samples were assayed for cytotoxicity and mineralized matrix formation. The anodized surfaces presented a higher rate of viable cells after 10 days, as well as a higher amount of nodules (p = 0.05). In conclusion, these results suggest that the nanotopography promoted by anodization using pulsed current induces beneficial modulatory effects on osteoblastic cells.

Keywords: Ti-6Al-4V alloy, anodizing, osseointegration, osteoblast activity.

1. Introduction

Currently, there has been growing interest in achieving osseointegration in shorter periods of time. In the past 40 years, titanium and its alloys, especially Ti-6Al-4V, have been considered the best choice as biomaterial for dental and orthopaedic implants and prosthesis, as they present good biological and mechanical properties [1, 2]. Aluminum and vanadium are alfa and beta stabilizers of titanium alloys, respectively, and they were selected so as to obtain a desirable microstructure and good mechanical properties. Despite these elements being associated with cytotoxicity [3, 4], researchers verified their ions, and found that they have an important function to a bone-forming cell. It can be possible that vanadium is a powerful element on maturing cells, although more studies are necessary [5]. As a result, recent researches on biomedical implants and biomaterials have focused their attention on developing materials which present surface characteristics that stimulate favourable cellular responses, as well as topographies that accelerate osseointegration [6, 7].

For improving the integration of an orthopedic implant with the bone tissue, various surface treatments for chemical and topographic modification of titanium have been considered. These include abrasion, polishing, etching, anodizing, among others. Surface properties of titanium implants are key factors as regards speed and stability of the implant integration with the bone. Surfaces with roughness in a micrometer scale are commonly prepared by sandblasting and acid etching. However, proteins and cells interact with the implant in a nanometer scale [8].

Anodizing electrochemical processes are based on the oxidation of metallic materials to form uniform and relatively thick films at room temperature [9]. Several metals and alloys undergo a spontaneous oxidation process when exposed to the atmosphere, thus leading to the formation of a very thin oxide layer on their surface [10]. Anodizing allows the obtainment of a relatively thin oxide layer that is denser than that which is naturally formed in the atmosphere. In the case of titanium and its alloys, this layer has been used to improve osseointegration [11].Researchers are particularly interested in this technique as it is a simple and easy method to manipulate experimental parameters in order to obtain microporous or nanoporous TiO_2 films. Determinate characteristics of the resulting oxide, such as the shape and size of pores, as well as their crystallinity, can promote cell nucleation and mechanical interlocking through bone growth in pores, thus leading to a more rapid osseointegration and implant stability within the body [12-16]. Experimental parameters that affect these surface characteristics are concentration, pH and temperature of the electrolyte, electric potential difference imposed between the cathode and the anode, the applied current density, and anodizing time [10, 17]. The thicker and more uniform layer can increase the corrosion resistance and abrasion from the implant and it is quite likely to improve osseointegration. [1, 13, 18-20]. Some researchers firmly believe that the crystalline structure of anodized TiO_2 has the potential to significantly affect its performance as a biomaterial [21]. In this sense, there are three crystalline forms of TiO_2: brookite, rutile and anatase; the latter being formed in lower temperatures and used in several application fields, including medical applications [22]. Anatase is known to have a higher electric conductivity than amorphous TiO_2, thus favouring charge transfer and the anodizing process. Furthermore, this crystalline form is less soluble in

physiological fluids than the amorphous form, consequently contributing to the resulting film's stability [23, 24]. In the present work, an anodic oxide film on the Ti-6Al-4V alloy was formed by using the pulsed current anodizing process. Then, osteoblast cells from calvarium bone neonate rats were inserted with anodized Ti-6Al-4V samples, and the effects of chemical composition, topography of the substrate on cytotoxicity, matrix mineralization, and formation of cellular cytoskeleton were studied.

2. Material and Methods

2.1. Sample preparation

The samples were prepared by using Ti-6Al-4V dowels measuring 1.1 cm in diameter. The dowels were cut into disc shapes measuring 0.3 cm by using an ISOMET 1000 precision cutter. Prior to the anodization, the samples were mechanically polished with SiC in the following granulations: 100, 200, 400 and 600 mesh. They were subsequently washed in ethanol for 10 min and a further 10 min in deionized water with an ultrasound device. Afterwards, they were polished in order to obtain mechanically reproducible surfaces. Twelve of the samples obtained in the previously described process were anodized in a 2.5 mol/L H_3PO_4 solution. Literature offers a multitude of possible combinations of anodizing parameters to obtain films with different structural characteristics. Generally speaking, anodic films on titanium grow with a crystalline structure at high potentials and with an amorphous structure at low potentials [24, 25]. However, in earlier studies, it has been demonstrated that it is possible to obtain crystalline films with the least potential (such as 10 or 30 V), since the anodization time is increased [25-27]. In this context, it was applied a pulse current of approximately 0.1 A cm^{-2} (100 Hz frequency, 15 min cycle, 40% efficiency per cycle) and maximum tension of 30 V. During the anodization process, the medium temperature varied between 21 and 23 °C. Then, the samples were washed in deionized water and left to dry in contact with air.

A digital oscilloscope (MO2061 model from Minipa), a square wave pulse rectifier (GI21P-10/30 model from General Inverter) and a multimeter (ET-2615A model from Minipa) were used to monitor the electrical parameters in the process. In the pulse current anodizing, three parameters can be adjusted: the duration of the current pulse (t_{on}), the time between current pulses (t_{off}) and the magnitude of the current pulse (i_p). The relation between t_{on} and t_{off} determines the duty cycle (dc) and frequency (f) of the process, defined as dc $= t_{on}/(t_{on} + t_{off})$ and $f = 1/(t_{on} + t_{off})$. In this work, the set parameters were only duty cycle and frequency. The control samples (group 1) and the anodized samples (group 2) were characterized using a ZEISS DSM 940 scanning electronic microscope and a Raman Horiba Scientific T64000 spectrometer at 514 nm.

2.2. Culture isolation and primary culture of osteogenic cells

All animal procedures were performed in accordance with the guidelines of the Research Ethics Committee of the School of Dentistry (UNESP) in São José dos Campos (027/2008-PA/CEP). Cells from newborn (2-4 days) Wistar rat's calvaria were harvested using the enzymatic digestion process that was previously

described by Oliveira and Nanci [28]. All samples were sterilized by Gamma radiation at 20 kGy (Embrarad, Empresa Brasileira de Radiações Ltda, Cotia, SP, Brazil) before cell culture. The cells were plated on the surfaces of samples from Groups 1 and 2 in 24-well polystyrene plates at cell density of 2 x 104 cells/well using α-MEM (Gibco-Life Technologies, NY, USA), supplemented with 10% fetal bovine serum (Gibco), 50 mg/mL gentamicin (Gibco), 5 µg/L ascorbic acid (Sigma, St. Louis, MO, EUA) and 7 mmol/L β-glycerophosphate (Sigma). During the experiment, the cells were incubated at 37ºC ± 1ºC in a humidified atmosphere of 5% CO_2, and the medium was changed every three days. The progress of cultures was examined by phase contrast microscopy (Model Axiovert 40C, Carl Zeiss Microscopy GmbH, Jena, Germany). Five samples from each group were used and all assays were conducted in triplicate.

2.3. MTT assay

The present method is based on a quantitative assessment of living cells after their exposure to a toxic agent or by experimental incubation with MTT dye [(bromide 3-4, 5-dimethylthiazol-2-yl) -2,5-difeniltetrazoliol] (Sigma). MTT is a salt which is reduced by mitochondrial proteinases that are active only in viable cells to produce a soluble formazan product in the culture medium. Then, a spectrophotometric analysis of the embedded dye is carried out, which is directly proportional to the number of cells living in the culture medium. In the cytotoxicity assay, a 0.2% phenol solution was used as positive control. To assess the cells' viability, they were grown in wells and evaluated in periods of 3 and 10 days. After being cultured in both periods, the MTT solution was added to the cells which were then incubated at 37ºC ± 1ºC for 4 h to form purple formazan crystals. Next, the supernatant was removed and the samples were washed with PBS, followed by the addition of 1 mL isopropanol acid (0.04 mol/L HCl in isopropanol) to each well so as to dissolve the formazan crystals. A colorimetric analysis was performed with an EL808IU spectrometer (Biotek Instruments, Winooski, VT, USA) at 650-570 nm. Data was expressed as absorbance.

2.4. Cell morphology

For the morphology analysis, the cells were cultured for 7 days. At 7 days, the cells were fixed for 10 min at 37ºC ± 1ºC using 4% paraformaldehyde in 0.1 mol/L phosphate buffer (PB) at pH 7.2. After being washed in PB, they were processed through direct fluorescence to verify the presence of cytoskeletons. The cells were then permeabilized with 0.5% Triton X-100 in PB for 10 min, followed by blocking unspecific background with 5% skimmed milk in PB for 30 min. A mixture of Alexa Fluor 488 (green fluorescence) and phalloidin (1:200, Molecular Probes Invitrogen) was incubated for 60 min in a humidified environment at room temperature. Before mounting for microscopic observation, the cells nuclei were stained with 300 nmol/L 4',6-diamidino-2-phenylindole dihydrochloride (DAPI, Molecular Probes Invitrogen) for 5 min, and the samples were briefly washed with distilled water subsequently. The samples were mounted using an antifade kit (Vectashield, Vector Laboratories, Burlingame, CA, USA). They were then examined under epifluorescence using a Leica DMLB light microscope (Leica, Bensheim, Germany) fitted with a Leica DC 300F digital camera.

2.5. Mineralized bone-like nodule formation

The formation of mineralized nodules was assessed after 14 days of culture. Afterwards, the wells were washed three times with Hank's solution (Sigma) at 37ºC ± 1ºC, and the cultures were fixed with 70% ethanol for 1 h at 4ºC. Following their fixation, they were washed twice with PBS and stained with 2% Alizarin red S (Sigma) at pH 4.2 for 15 min at 37ºC ± 1ºC. This solution stains mineralized matrix nodules. The samples were washed three times with deionized H_2O and left to dry for 24 h at 37ºC ± 1ºC. To quantify the formation of mineralized nodules, 560 μL of 10% acetic acid was added to each well and, to neutralize the acid, 40 μL of 10% ammonia hydroxide was subsequently added. The reading was performed at 405 nm in a spectrometer. The values were expressed as optical density.

2.6. Statistical analysis

The statistical analysis was performed using a nonparametric test, for independent data (Kruskal-Wallis), followed by a multiple comparison test whenever applicable (Dunn). The significance level was 5%. The results are representative of experiments performed with three distinct primary cultures.

3. Results and Discussion

3.1. Sample characterization

Figure 1 shows oscilloscope data on the current pulse applied during the anodization of the twelve samples of commercial Ti-6Al-4V alloy. These samples were subsequently assessed for cellular viability. According to the data collected, current pulses ranged from 400 to 700 mA, whilst the tension remained constant at 30 V. This variation may be due to small differences between the mechanically polished surfaces which exhibit different susceptibility to oxidation and film growth.

Figure 2 shows the SEM images with the same magnification (1000 X). The micrographs reveal that the anodizing by pulsed current induces strong morphological variations during film formation. An apparently uniform distribution of different pore sizes (≤ 5 μm) was observed.

Figure 3 shows the Raman spectrum of the formed film, displaying three bands positioned between 400 and 700 cm^{-1}, which may be attributed to the crystalline structure of TiO_2 anatase [29]. However, the peak indicated at approximately 158 cm^{-1} is usually associated with amorphous TiO_2 oxide, which is opposed to the peak that is typically seen in crystalline anatase, which occurs at around 147 cm^{-1}, as reported by several authors [30-33]. However, Liu et al. [29] have attributed this intense peak at 158 cm^{-1} to the anatase. Raman spectra of thin films on various substrates anatase were obtained by these authors, wherein the bands' frequencies were identified as: 147 (± 2.8) cm^{-1}, 392.8 (± 4.3) cm^{-1}, 515.2 (± 5.3) cm^{-1}, 513.14 (± 7.4) cm^{-1} 628.8 (±10.2) cm^{-1}.
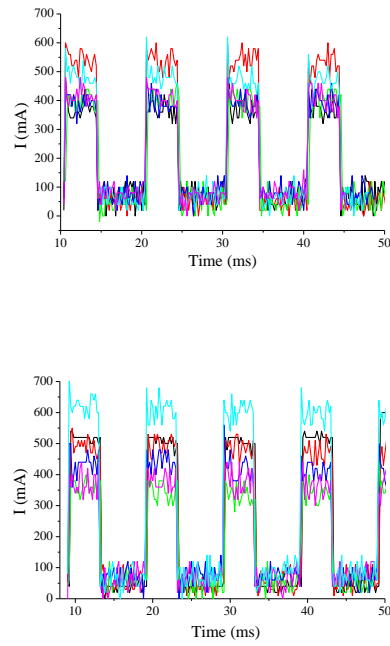
**Fig. 1. Oscilloscope data showing current pulses
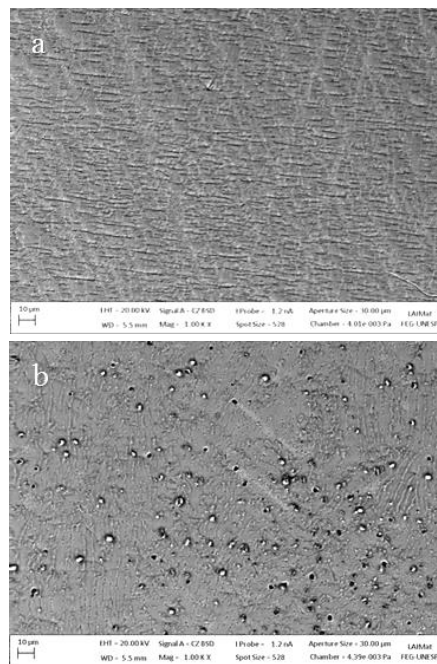applied during the anodization of the twelve Ti-6Al-4V samples.**

**Fig. 2. Ti-6Al-4V micrographs obtained using SEM:
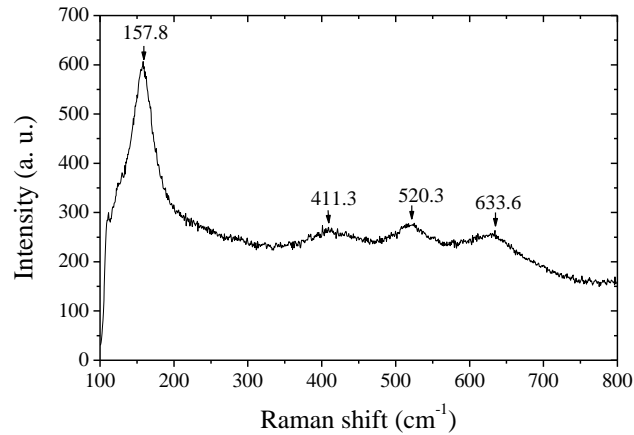(a) before; (b) after pulsed current anodization.**

Fig. 3. Raman spectrum obtained for one of the twelve anodized samples.

3.2. *In vitro* tests

3.2.1. MTT assay

Cell viability has gradually increased in all groups over time; i.e. the cells continue to grow over time, indicating that none of the samples were toxic. ANOVA results showed no statistically significant difference in cell viability after 3 and 10 days of culture ($p > 0.05$), both in G1 and G2. However, the descriptive statistical analysis demonstrated that the anodized samples presented better results in both studied periods; i.e. the mean number of viable cells of anodized samples was higher than the other groups of samples. At 3 days, the values of G1 and G2 were 0.038 and 0.055 respectively, and 0.124 and 0.128 at 10 days. An increase in cell viability was seen as time progressed, with a statistical difference observed between the periods ($p < 0.05$). At 10 days, the anodized samples presented the highest viable cell counts.

3.2.2. Cell morphology

Randomized cell spreading occurred on all surfaces. Irrespective of material composition, dense samples presented a large number of cells in both groups. Figure 4(a) shows that the anodized samples presented a greater number of cells with a more elongated shape, whilst there was less cell density in the control group. Figure 4(b) shows a porous surface with stellate polygonal morphology and multidirectional spreading. Cell nuclei are shown in blue and cytoskeletons in green by Direct Fluorescence, Alexa Fluor 488, phalloidin and DAPI.

3.2.3. Mineralized bone-like nodule formation

As regards the mineralization nodules at 14 days, it was observed that group 1 exhibited mean absorbance value of 0.088, while group 2 showed a value of 0.063, not being a statistically significant difference ($p > 0.05$).

Nodule formation at 14 days was neither affected by the material, nor by surface topography. Group 1 showed a mean absorbance value of 0.088, whereas group 2 obtained a value of 0.063, which is not a statistically significant difference (p>0.05).
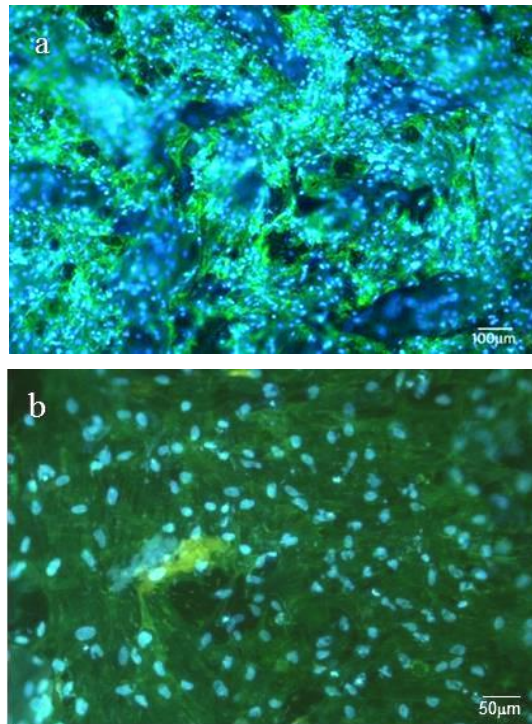

Fig. 4. (a) Cell spreading in anodized samples: more cells and more numerous elongated shapes; (b) Cell nuclei are shown in blue, while cytoskeletons in green.

In the *in vitro* tests of the present study, it was observed that the cell viability increased in the treated samples, but without showing a significant statistical difference, suggesting better cellular response to anodized surfaces and indicating that the parameters used for anodizing did not exhibit cytotoxicity. Therefore, it was concluded that the chemical composition and topography of the anodized surface promoted osteogenesis and cell viability, corroborating with findings from previous studies [24-37].

This study described and assessed an anodic electrochemical process that resulted in TiO_2 formation. Pores were found in the TiO_2 layers, which stimulated the absorption of proteins and the recruitment of osteoblasts in comparison with the control group. The increased number of viable cells observed in this study could be attributed to the presence of pores, as this would provide a larger surface area available for cell growth, which is associated with modifications in the surface chemical composition, as the achievement of anatase phase.

Several authors have previously shown that osteoblast cell adhesion and orientation, as well as faster osseointegration occur in anodized surfaces [38-42]. This is possibly due to the crystalline aspect of the TiO_2 film, and it can be associated with open and irregular shaped pores that emerge on the implant surface during the anodization. These pores resemble the shape of volcanoes, with 1 to 2 μm mean diameter [36, 39, 42]. This type of surface presents an integral topography, absence of acute characteristics and good capacity for retaining liquids and bone tissue, according to the consulted literature [43-46].

It was observed that the anodization of the samples strongly affected the cellular cytoskeleton. Cell spreading was greater on the anodized samples than in the control group. This behavior can be explained by the chemical attraction of the anatase layer. Sjöström et al. [45] reported that anodized Ti surfaces have enhanced cellular adhesion, dissemination, cytoskeleton formation and cellular differentiation, which is probably due to a more hydrophilicity feature of the TiO_2 crystalline phase, such as anatase features.

Cell differentiation can be assessed by cell spreading, filopodia extension, cell density, and also mineralization nodule formation. The amount of mineralization nodules formed in the anodized group was less prominent, and similar to what was observed in the control group, suggesting that cell differentiation happened in both groups. According to Pereira et al. [47], the delay in cell differentiation on experimental surfaces could suggest that terminal osteoblastic differentiation on modified surfaces would not necessarily depend on cell multilayering that takes place after the confluence on flat, dense substrates, and precedes and colocalizes with nodule formation in calvarial cell cultures.

4. Conclusions

The anodization process by pulsed current plays an important role in modifying implant surfaces, as it enhances cellular response, indicates an increase of cells, and brings benefits in medical and dental clinics. These findings reveal that the development of modified structures with a new surface, such as the anodized Ti-6Al-4V surface demonstrated in this study, should enable better osseointegration and cell-implant. Furthermore, it indicates that the anodization parameters (pulse current of 0.1 $A \, cm^{-2}$, 100 Hz frequency, 15 min cycle, maximum tension of 30 V, and 2.5 mol L^{-1} phosphoric acid) improve bone formation and can be used in the development of implants to be utilized in surgical procedures. Therefore, more studies, especially *in vivo*, should be conducted to confirm the results obtained from this research.

References

1. Niinomi, M.; Nakai, M.; Hieda, J. (2012). Development of new metallic alloys for biomedical applications. *Acta Biomaterialia*, 8(11), 3888-3903.

2. Schneider, S.C. (2001). *Obtaining and characterizing the Ti-13Nb-13Zr alloy for application as a biomaterial*. Ph.D. Thesis. Institute of Energy and Nuclear Research, Rio de Janeiro, Brazil.

3. Huang, H.H.; Wu, C.P.; Sun, Y.S.; Yang, W.E.; Lee, T.H. (2014). Surface nanotopography of an anodized Ti-6Al-7Nb alloy enhances cell growth. *Journal of Alloys and Compounds*, 615(1), S648-S654.

4. Yang, Y.; Serpersu, K.; He, W.; Paital, S.R.; Dahotre, N.B. (2011). Osteoblast interaction with laser cladded HA and SiO2-HA coatings on Ti-6Al-4V. *Materials Science and Engineering C*, 31(8), 1643-1652.

5. Ku, C.H.; Pioletti, D.P.; Browne, M.; Gregson, P. J. (2002). Effect of different Ti-6Al-4V surface treatments on osteoblasts behaviour. *Biomaterial*s, 23(6), 1447-1454.

6. Lee, W.F.; Yang, T.S.; Wu, Y.C.; Peng, P.W. (2013). Nanoporous biocompatible layer on Ti-6Al-4V alloys enhanced osteoblast-like cell response**.** *Journal of Experimental & Clinical Medicine*, 5(3), 92-96.

7. Duarte, L.T.; Bolfarini, C.; Biaggio, S.R.; Rocha-Filho, R.C.; Nascente, P.A. (2014). Growth of aluminum-free porous oxide layers on titanium and its alloys Ti-6Al-4V and Ti-6Al-7Nb by micro-arc oxidation. *Materials Science and Engineering C: Materials for Biological Application*, 1(41), 343-348.

8. Salou, L.; Hoornaert, A.; Louarn, G.; Layrolle, P. (2015). Enhanced osseointegration of titanium implants with nanostructured surfaces: an experimental study in rabbits. *Acta Biomaterialia*, 11(1), 494-502.

9. Narayanan, R., Seshadri, S.K. (2007). Phosphoric acid anodization of Ti-6Al-4V - Structural and corrosion aspects. *Corrosion Science*, 49(2), 542-558.

10. Diamanti, M.V.; Pedeferri, M.P. (2007). Effect of anodic oxidation parameters on the titanium oxides formation. *Corrosion Science*, 49(2), 939-948.

11. Kim, S.E.; Lim, J.H.; Lee, S.C.; Nam, S.; Kang, H.; Choi, J. (2008). Anodically nanostructured titanium oxides for implant applications. *Electrochimica Acta*, 53(14), 4846-4851.

12. Ketabchi, A.: Weck, A.; Variola, F. (2015). Influence of oxidative nanopatterning and anodization on the fatigue resistance of commercially pure titanium and Ti6Al4V. *Journal of Biomedical Materials Science*, 103(3), 563-571.

13. Sul, Y.T.; Johansson, C.B.; Petronis, S. ; Krozer, A. ; Jeong, Y. ; Wennerberg, A. ; and Albrektsson, T. (2002). Characteristics of the surface oxides on turned and electrochemically oxidized pure titanium implants up to dielectric breakdown: the oxide thickness, micropore configurations, surface roughness, crystal structure and chemical composition. *Biomaterials*, 23(2), 491-501.

14. Sista, S.; Nouri, A.; Li, Y.; Wen, C.; Hodgson, P.D.; Pande, G. (2013). Cell biological responses of osteoblasts on anodized nanotubular surface of a titanium-zirconium alloy. *Journal of Biomedical Materials Research*, 101(12), 3416-3430.

15. Albrektsson, T.; Wennerberg, A. (2004). Oral implant surfaces: part 1 review focusing on topographic and chemical properties of different surfaces and in vivo responses to them. *International Journal of Prosthodontics*, 17(5), 536-543.

16. Sul, Y.T.; Johansson, C.; Byon, E.; Albrektsson, T. (2005). The bone response of oxidized bioactive and non-bioactive titanium implants. *Biomaterials*, 26(33), 6720-6730.

17. Adamek, G.; Jakubowicz, J. (2010). Mechanoelectrochemical synthesis and properties of porous nano-Ti-6Al-4V alloy with hydroxyapatite layer for biomedical applications. *Electrochemistry Communications*, 12(5), 653-656.

18. Parr, G.R.; Gardner, L.K.; Toth, R.W. (1985). Titanium: the mystery metal of implant dentistry: dental materials aspects. *Journal of Prosthetic Dentistry*, 54(3), 410-414.

19. Kasemo, B.; Lausmaa, J. (1983). Aspect of surface physics on titanium implants. *Swedish Dental Journal*, 28, 19-36.

20. Zitter, H.; Plenk, H.J. (1987). The electrochemical behavior of metallic implant materials as indicator of their biocompatibility. *Journal of Biomedical Materials Research*, 21(7), 881-896.

21. Willianson, R.S.; Disegi, J.; Griggs, J.A.; Roach, M.D. (2013). Nanopore formation on the surface oxide of commercially pure titanium grade 4 using a pulsed anodization method in sulfuric acid. *Journal of Materials Science: Materials in Medicine*, 24(10), 2327-2335.

22. Doroudian, G.; Curtis, M.W.; Gang, A.; Russell, B. (2013). Cyclic strain dominates over microtopography in regulating cytoskeletal and focal adhesion remodeling of human mesenchymal stem cells. *Biochemical and Biophysical Research Communications*, 430(3), 1040-1046.

23. Simka, W.; Sadkowski, A.; Warczak, M.; Iwaniak, A.; Dercz, G.; Michalska, J.; Maciej, A. (2011). Characterization of passive films formed on titanium during anodic oxidation. *Electrochimica Acta*, 56(24), 8962-8968.

24. Diamanti, M.V.; Ormellese, M,; Pedeferri, M.P. (2010). Alternating current anodizing of titanium in halogen acids combined with anodic spark deposition: morphological and structural variations. *Corrosion Science*, 52(5), 1824-1829.

25. Xing, J.; Xia, Z.; Hu, J.; Zhang, Y.; Zhong, L. (2013). Time dependence of growth and crystallization of anodic titanium oxide films in potentiostatic mode. *Corrosion Science*, 75, 212-219.

26. Mizukoshi, Y.; Ohtsu, N.; Masahashi, N. (2013). Structural and characteristic variation of anodic oxide on pure Ti with anodization duration. *Applied Surface Science*, 283, 1018-1023.

27. Díaz, P.L.; Pereira, M.C.; Codaro, E.N.; Acciari, H.A. (2016). Structural changes in TiO2 films formed by anodizing of electro-polished titanium. *Materials Science Forum*, in press.

28. Oliveira, P.T.; Nanci, A. (2004). Nanotexturing of titanium-based surfaces upregulates expression of bone sialoprotein and osteopontin by cultured osteogenic cells. *Biomaterials*, 25(3), 403-413.

29. Liu, J.H.: Yi, J.L.; Li, S.M.; Yu, M.; Xu, Y.Z. (2009). Fabrication and characterization of anodic films on a Ti-10V-2Fe-3Al titanium alloy. *International Journal of Minerals, Metallurgy and Materials*, 16(1), 96-100.

30. Jaeggi, C.; Parlinska-Wojtan, M.; Kern, P. (2012). Correlation of electrolyte-derived inclusions to crystallization in the early stage of anodic oxide film growth on titanium. *Thin Sol Films*, 520(6), 1804-1808.

31. Khadar, M.A.; Shanid, N.A.M. (2010). Nanoscale fine-structure evaluation of RF magnetron sputtered anatase films using HRTEM, AFM, micro-Raman

spectroscopy and fractal analysis. *Surface & Coatings Technology*, 204(9-10), 1366-1374.

32. Vasconcellos, L.M.R.; Oliveira, F.N.; Leite, D.O.; Vasconcellos, L.G.O.; Prado, R.F.; Ramos, C.J.; Graça, M.L.A.; Cairo, C.A.A.; Carvalho, Y.R. (2012). Novel production method of porous surface Ti samples for biomedical application. *Journal of Materials Science: Materials in Medicine*, 23(2), 357-364.

33. Niinomi, M. (2008). Mechanical biocompatibilities of titanium alloys for biomedical applications. *Journal of Mechanical Behavior of Biomedical Materials*, 1(1), 30-42.

34. Sugita, Y.; Ishizaki, K.; Iwasa, F.; Ueno, T.; Minamikawa, H.; Yamada, M.; Suzuki, T.; Ogawa, T. (2011). Effects of pico-to-nanometer-thin TiO_2 coating on the biological properties of microroughened titanium. *Biomaterials*, 32(33), 8374-8384.

35. Park, J.W.; Park, K.B.; Suh, J.Y. (2007). Effects of calcium ion incorporation on bone healing of Ti6Al4V alloy implants in rabbit tibiae. *Biomaterials*, 28(22), 3306-3313.

36. Elias, C.N.; Serra, L.E. (2006). Titanium biocompatibility and the *vulcano* surfasse. Revista *Brasileira de Implantodontia*, 12(3), 6-11.

37. Lavenus, S.; Trichet, V.; Le Chevalier, S.; Hoornaert, A.; Louarn, G.; Layrolle, P. (2012). Cell differentiation and osseointegration influenced by nanoscale anodized titanium surfaces. *Nanomedicine*, 7(7), 967-980.

38. Zuo, J.; Huang, X.; Zhong, X.; Zhu, B.; Sun, Q.; Jin, C.; Quan, H.; Tang, Z.; Chen, W. (2013). A comparative study of the influence of three pure titanium plates with different micro- and nanotopographic surfaces on preosteoblast behaviors. *Journal of Biomedical Materials Research Part A*, 101(11), 3278-3284.

39. Liang, D., Hsiao, B.S.; Chu, B. (2007). Functional electrospun nanofibrous scaffolds for biomedical applications. *Advanced Drug Delivery Reviews*, 59(14), 1392-1412.

40. Al-Nawas, B.; Grotz, K. A.; Goetz, H..; Feil, M.; Duschner, H.; Wagner, W. (2006). Systematische qualitative Histologie von enossalen Implantaten mit anodisch oxidierten. *Oberflächen Mund-, Kiefer- und Gesichtschirurgie*, 10(4), 229-237.

41. Li, Y.; Gao, Y.; Shao, B.; Xiao, J.; Hu, K.; Kong, L. (2012). Effects of hydrofluoric acid and anodised micro and micro/nano surface implants on early osseointegration in rats. *British Journal of Oral and Maxillofacial Surgery*, 50(8), 779-783.

42. Xiao, J.; Zhou, H.; Zhao, L.; Sun, Y.; Guan, S.; Liu, B.; Kong, L. (2011). The effect of hierarchical micro/nanosurface titanium implant on osseointegration in ovariectomized sheep. *Osteoporosis International*, 22(6), 1907-1913.

43. Kim, Y.H.; Koak, J.Y.; Chang, I.T.; Wennerberg, A.; Heo, S.J. (2003). A histomorphometric analysis of the effects of various surface treatment methods on osseointegration. *International Journal of Oral Maxillofacial Implants*, 18(3), 349-356.

44. Yu, X.; Li, Y.; Wlodarky, W.; Kandasamy, S.; Kalantar-Zadeh, K. (2008). Fabrication of nanostructured TiO_2 by anodization: a comparison between electrolytes and substrates. *Sensors and Actuators* B: Chemical 130(1), 25-31.

45. Sjöström, T.; Dalby, M.J.; Hart, A.; Tare, R.; Oreffo, R.O.; Su, B. (2009). Fabrication of pillar-like titania nanostructures on titanium and their interactions with human skeletal stem cells. *Acta Biomaterialia*, 5(5), 1433-1441.

46. Han Pei, J.I.; Wei, P.; Zhao, C.; Zhang, X.; Jiang, Y. (2011). Improved osteoblast proliferation, differentiation and mineralization on nanophase Ti6Al4V. *Chinese Medical Journal*, 124(2), 273-279.

47. Pereira, K.K.Y.; Alves, O.C.; A.O.C.; Novaes Jr., A.B.; Oliveira, F.S.; Yi, J.H.; Zaniquelli, O.; Wolf-Brandstetter, W.; Scharnweber, D.; Variola, F.; Nanci, A.; Rosa, A.L.; Oliveira, P.T. (2013). Progression of osteogenic cell cultures grown on microtopographic titanium coated with calcium phosphate and functionalized with a type I collagen-derived peptide. *Journal of Periodontology*, 84(8), 1199-1210.